CHEST

Special Features

CHEST IMAGING

A Practical Algorithmic Approach to the Diagnosis and Management of Solitary Pulmonary Nodules

Part 1: Radiologic Characteristics and Imaging Modalities

Vishal K. Patel, MBBS; Sagar K. Naik, MBBS; David P. Naidich, MD, FCCP; William D. Travis, MD, FCCP; Jeremy A. Weingarten, MD, FCCP; Richard Lazzaro, MD; David D. Gutterman, MD, FCCP; Catherine Wentowski, MD; Horiana B. Grosu, MD; and Suhail Raoof, MBBS, FCCP

The solitary pulmonary nodule (SPN) is frequently encountered on chest imaging and poses an important diagnostic challenge to clinicians. The differential diagnosis is broad, ranging from benign granulomata and infectious processes to malignancy. Important concepts in the evaluation of SPNs include the definition, morphologic characteristics via appropriate imaging modalities, and the calculation of pretest probability of malignancy. Morphologic differentiation of SPN into solid or subsolid types is important in the choice of follow-up and further management. In this first part of a two-part series, we describe the morphologic characteristics and various imaging modalities available to further characterize SPN. In Part 2, we will describe the determination of pretest probability of malignancy and an algorithmic approach to the diagnosis of SPN.

CHEST 2013; 143(3):825–839

Abbreviations: ATS = American Thoracic Society; ERS = European Respiratory Society; FDG = ^{18}F-2-deoxy-2-fluoro-D-glucose; GGN = ground glass nodule; IASLC = International Association for the Study of Lung Cancer; NPV = negative predictive value; NSCLC = non-small cell lung cancer; PPV = positive predictive value; SPN = solitary pulmonary nodule; SUV = standardized uptake value

The solitary pulmonary nodule (SPN) is defined as a radiographic opacity ≤ 3 cm in diameter with at least two-thirds of its margins surrounded by lung parenchyma.[1,2] Implied in this definition is the exclusion of lymph nodes, atelectasis, and postobstructive pneumonia. However, it may be difficult at times to exclude intraparenchymal lymph nodes based on just radiologic appearance. SPNs have been noted in 0.09% to 7% of all chest radiographs.[3-5] A review of eight large studies on lung cancer screening using CT imaging[6-13] documented the prevalence of SPN from 8% to 51%, and the prevalence of malignancy from 1.1% to 12%.[14] The etiologic spectrum of SPN represents a veritable minefield of diseases, including benign conditions such as hamartomas to potentially fatal ones such as primary lung cancer (Table 1). Establishing the etiology of a SPN in a timely and accurate manner, therefore, assumes critical importance, since surgical resection in a patient with early-stage lung cancer provides the highest chance of cure. By the same token, avoiding thoracic surgery for a benign SPN whenever possible does obviate significant morbidity. We will describe an algorithmic approach to diagnosis of SPN in Part 2 (see page 840).[15]

Clinical Evaluation

A SPN does not typically herald its presence with clinical symptoms, nor does it lend itself to self-awareness like melanoma or a breast lump. Although the SPN may be insidious, a variety of clinical risk factors such as advancing age and history of smoking have been associated with a higher OR of the SPN being malignant.[15-19] Elucidating a thorough history of prior malignancy is crucial; the majority of SPNs detected in patients with a history of prior malignancy are malignant.[20-22] Interestingly, the malignant SPNs are equally or more likely to represent primary lung cancer rather

than metastasis from the extrapulmonary malignancy, with the notable exceptions of sarcoma, melanoma, and testicular carcinoma (Table 2). The presence of mediastinal lymph node enlargement on CT scan strongly suggests a new primary lung cancer rather than metastasis.[20] Interstitial lung diseases, such as idiopathic pulmonary fibrosis, asbestosis, and scleroderma are associated with an increased incidence of lung cancer.[23] The prevalence of lung cancer in idiopathic pulmonary fibrosis, for example, ranges from 9% to 38%, with a predilection for peripheral lung areas in the lower lobes in elderly male smokers.[24-29] Finally, residence in or travel to an area with endemic fungal pathogens could suggest a benign, infectious SPN in the correct clinical context. For example, coccidioidomycosis is endemic in the southwestern United States and Mexico, and often presents as a SPN on chest CT scans.[30] *Cryptococcus*[31-33] infection and histoplasmosis can also present as a SPN.

Radiographic Characteristics: CT Scan

Specific morphologic characteristics of SPNs on imaging may help differentiate benign from malignant SPNs. It is recommended that CT images be thin section, with contiguous 1-mm images through nodules. Both lung and mediastinal windows should be obtained, the former for the edges, the latter for solid components. Low-dose (milliamperes second [mAs] <80) CT scan can be used for this purpose.

Growth Rate

Malignant, solid SPNs have a volume doubling time of 20-400 days,[34-38] with a majority having volume doubling times of significantly <100 days.[39] A volume doubling time >400 days suggests slow growth and is usually associated with benign SPNs, whereas volume doubling time <20 days indicates very rapid growth, usually attributable to infectious processes.[40] It is important to realize that since the volume of a sphere equals $4\pi r^3/3$, an increase in nodule diameter by only 26% indicates doubling of volume. In other words, a

Table 1—*Differential Diagnosis of Solitary Pulmonary Nodules*

Infectious
TB (tuberculoma)
Round pneumonia, organizing pneumonia
Lung abscess
Fungal: aspergillosis, blastomycosis, cryptococcosis, histoplasmosis, coccidioidomycosis
Parasitic: amoebiasis, echinococcosis, *Dirofilaria immitis* (dog heartworm)
Measles
Nocardia
Atypical mycobacteria
Pneumocystis jiroveci
Septic embolus
Neoplastic
Benign
Hamartoma
Chondroma
Fibroma
Lipoma
Neural tumor (Schwannoma, neurofibroma)
Sclerosing hemangioma
Plasma cell granuloma
Endometriosis
Malignant
Lung cancer
Primary pulmonary carcinoid
Solitary metastasis
Teratoma
Leiomyoma
Vascular
Arteriovenous malformation
Pulmonary infarct
Pulmonary artery aneurysm
Pulmonary venous varix
Hematoma
Congenital
Bronchogenic cyst
Lung sequestration
Bronchial atresia with mucoid impaction
Inflammatory
Rheumatoid arthritis
Granulomatosis with polyangiitis (Wegener)
Microscopic polyangiitis
Sarcoidosis
Lymphatic
Intrapulmonary or subpleural lymph node
Lymphoma
Outside lung fields
Skin nodule
Nipple shadows
Rib fracture
Pleural thickening, mass or fluid (pseudotumor [ie, loculated fluid])
Miscellaneous
Rounded atelectasis
Lipoid pneumonia
Amyloidosis
Mucoid impaction (mucocele)
Infected bulla
Pulmonary scar

Manuscript received June 12, 2012; revision accepted October 10, 2012.
Affiliations: From the New York Methodist Hospital (Drs Patel, Naik, Weingarten, Lazzaro, Wentowski, Grosu, and Raoof), Brooklyn, NY; New York University Langone Medical Center (Dr Naidich), New York, NY; Memorial Sloan-Kettering Cancer Center (Dr Travis), New York, NY; and Medical College of Wisconsin (Dr Gutterman), Milwaukee, WI.
Correspondence to: Suhail Raoof, MBBS, FCCP, New York Methodist Hospital, Department of Pulmonary and Critical Care, 506 Sixth St, Brooklyn, NY 11215; e-mail: suhailraoof@gmail.com

DOI: 10.1378/chest.12-0960

Table 2—*Extrapulmonary Malignancy and Ratio of Primary vs Metastatic SPNs*[20-22]

Extrapulmonary Malignancy	Ratio of Malignant SPNs Representing Primary Lung Cancer vs Metastasis From the Extrapulmonary Malignancy
Carcinomas of the head and neck	25:3
Cancers of the bladder, breast, cervix, bile ducts, esophagus, ovary, prostate, or stomach	26:8
Cancers of the salivary glands, adrenal gland, colon, parotid gland, kidney, thyroid gland, thymus, or uterus	13:16
Melanoma, sarcoma, or testicular carcinoma	9:23

SPN = solitary pulmonary nodule. See text for explanation.

4-mm nodule may double in volume, but its size will barely increase to 5 mm, a change often too subtle to detect reliably on CT scans.[41] Three-dimensional volumetric measurement of a SPN on a CT scan of the chest can provide a more accurate assessment of growth rate compared with the SPN diameter, especially in small (< 1 cm) SPNs (Fig 1).[42-44] However, it must be pointed out that there is significant controversy regarding the most accurate method to follow the rate of growth of nodules. There are those who advocate for volumetric analysis, but this is generally applicable for solid lesions > 8 to 10 mm. The data for smaller lesions are less compelling. It should also be stated that for ground glass and subsolid nodules, assessment of growth rate is even less clear. These lesions may be followed by assessing their mass, that is, a combination of both volume and density.[45,46] To date, there is no consensus on the best way to follow these lesions. In general, a solid SPN, stable in volume over a period of 2 years (which indicates a doubling time > 730 days) can be reliably considered benign; important exceptions to this rule are slow-growing adenocarcinomas of the lung, especially those presenting as pure ground glass nodules (GGNs), as will be discussed separately.

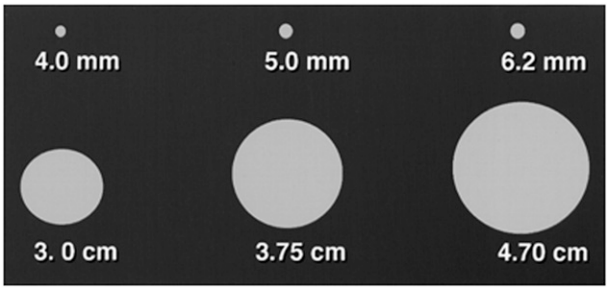

FIGURE 1. Solitary pulmonary nodule (SPN) doubling time. A 4-mm nodule can double in size over a period of time but the diameter will increase only approximately 1 mm to 5 mm, which may not be reliably detected on the CT scan. However, an increase in a bigger mass is very well appreciated by just looking at the diameter on the CT scan.

Size

The likelihood of malignancy in a SPN increases with the nodule diameter[47,48](Fig 2). Lesions larger than 3 cm are more likely to be malignant. However, a smaller size does not exclude malignancy.

Location

SPNs in the upper lobes have been observed to be malignant in a larger number of cases.[17,49,50] This is possibly because there is a higher concentration of inhaled carcinogens in the upper lobes resulting from cigarette smoking.[40]

Margin/Border/Edge Characteristics

Furuya et al[51] divided margins of SPNs into seven categories: smooth, lobulated, spiculated, ragged, tentacle, polygonal, and with surrounding halo and with notches or concavity. The described margin types and their possible etiologies are shown in Table 3 and Figures 3-8.[16,47,51-59]

Calcification and Attenuation

Specific patterns of calcification within a SPN (diffuse, central [bull's eye], laminated or concentric, or popcorn) can suggest a benign lesion (Figs 9-12). However, there is no pattern of calcification that is considered specific for malignancy[60] (Table 4[40,61-65]). The plain chest roentgenogram is not very sensitive in detecting calcification within a SPN, demonstrating a sensitivity of 50% and a specificity of 87%.[66,67] Hence, a noncontrast CT scan with 1 to 3 mm sections through the nodule is recommended to assess the SPN and the calcification within the SPN. Attenuation values > 200 Hounsfield units in a SPN indicate the presence of calcium in the nodule.[68]

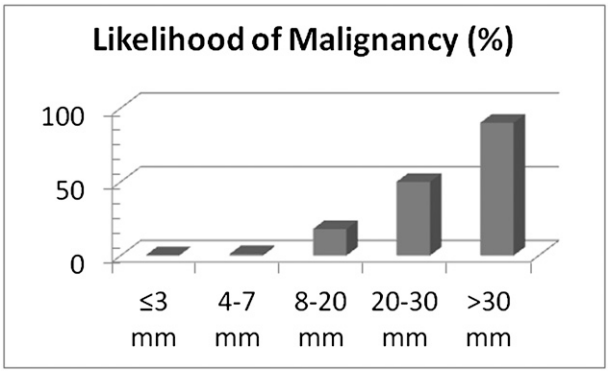

FIGURE 2. SPN size and corresponding likelihood of malignancy. See Figure 1 legend for expansion of abbreviation.

Table 3—*Margin Characteristics of SPNs*

Margin	Etiology
Smooth	Suggests a benign lesion. However, may be malignant in up to one-third of cases.[50,52]
Lobulated	Suggests uneven growth; a PPV of 80% for malignancy.[45,49] Up to 25% of benign lesions, such as hamartomas, can have lobulated margins.[51]
Spiculated	A spiculated margin (the so-called corona radiata sign) is highly predictive of malignancy, with a PPV of 88% to 94%.[16,49,50,53] A few exceptions of benign SPNs that could have spiculated margins include lipoid pneumonia, focal atelectasis, tuberculoma, and progressive massive fibrosis.[45,54]
Ragged	Suggests growth pattern along the alveolar wall; lepidic pattern of adenocarcinoma.
Tentacle or polygonal	Seen in fibrosis, alveolar infiltration, and collapsed alveoli.[49]
Halo	SPN surrounded by a "halo" of ground glass attenuation, also called the "CT halo sign." Seen in aspergillosis, Kaposi sarcoma, granulomatosis with polyangiitis (Wegener), and metastatic angiosarcoma.[55,56] Adenocarcinoma in situ (previously known as bronchoalveolar carcinoma) can also produce a halo, due to its lepidic growth.
Notches	SPN with notches or concavity in the margin is seen in some SPNs with tumor growth. These notches are frequently found in adenocarcinomas with overt invasion and are associated with poor prognosis.[57]

PPV = positive predictive value. See Table 2 legend for expansion of other abbreviation.

Fat

An attenuation value of a SPN between −40 and −120 Hounsfield units suggests the presence of fat, which is present in up to 60% of hamartomas[52,69] (Fig 13). Rare causes of fat attenuation include lipoid pneumonia and pulmonary metastases from liposarcoma (almost always solid-appearing lesions), and renal cell carcinoma.[70,71]

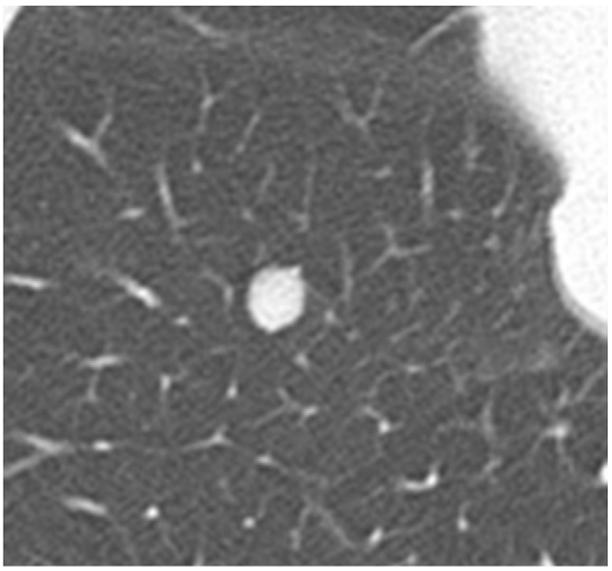

FIGURE 3. SPN with a smooth border. A SPN with smooth borders may suggest benign etiology, although up to one-third of these lesions can be malignant. See Figure 1 legend for expansion of abbreviation.

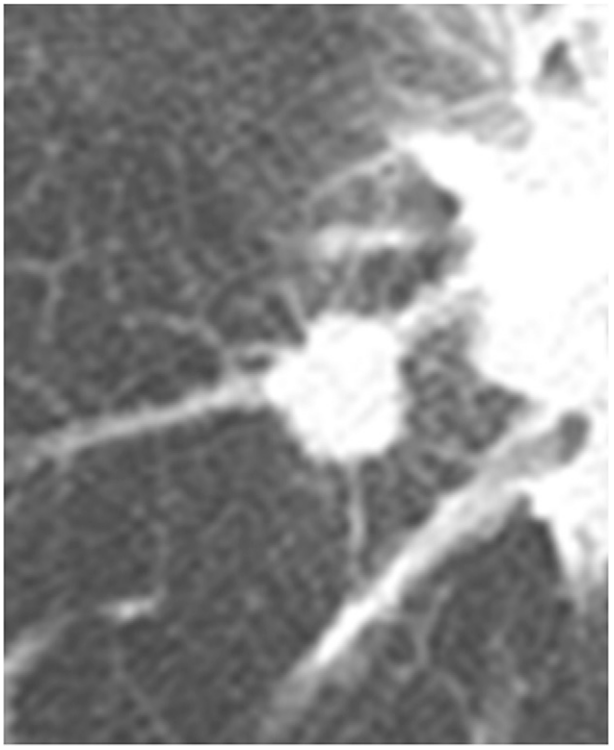

FIGURE 4. SPN with lobulated margin suggests uneven growth and likely is malignant with a positive predictive value of 80%. Up to 25% of benign lesions such as hamartomas can have lobulated margins. See Figure 1 legend for expansion of abbreviation.

Cavitation

Cavitation can be seen in necrotic malignant SPNs like squamous cell carcinoma, as well as benign SPNs such as abscesses, infectious granulomas, vasculitides, early Langerhans cell histiocytosis, and pulmonary infarction. Cavity wall thickness <5 mm points toward a benign etiology, whereas irregular and thicker walls >15 mm are seen with malignant lesions, although this is not always true (Fig 14).[72,73] Small lucencies in a SPN may be seen in adenocarcinomas in situ or lepidic predominant adenocarcinomas (both previously known as bronchoalveolar carcinoma) (Figs 15, 16).[74,75] This pattern, often referred to as "bubbly lucencies," can also be seen in pulmonary lymphoma, sarcoidosis, round pneumonia, and organizing pneumonia.[70,76,77] Sometimes, fluid-filled lesions from mucus impaction can appear as cavitating SPN.

Ground Glass Nodules

Pulmonary nodules can be characterized on CT scan as either solid or subsolid. Solid nodules completely

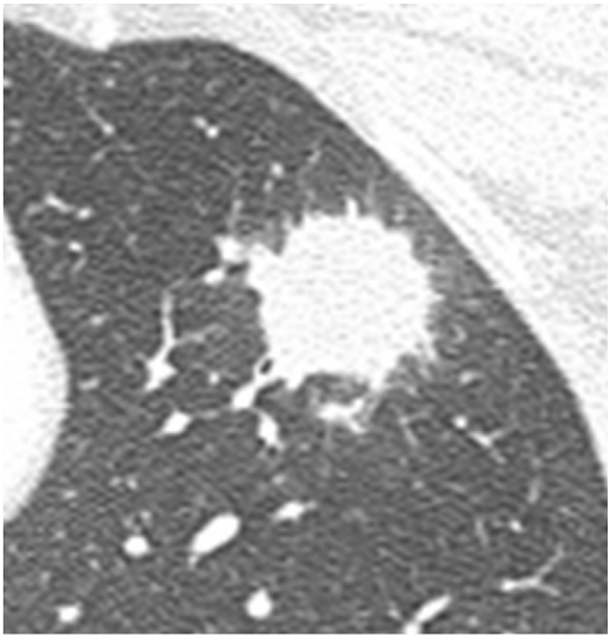

FIGURE 5. SPN with spiculated margin (corona radiata sign). This is highly predictive of malignancy with a positive predictive value of 88% to 94%. Lipoid pneumonia, focal atelectasis, tuberculoma, and progressive massive fibrosis can have spiculated margins. See Figure 1 legend for expansion of abbreviation.

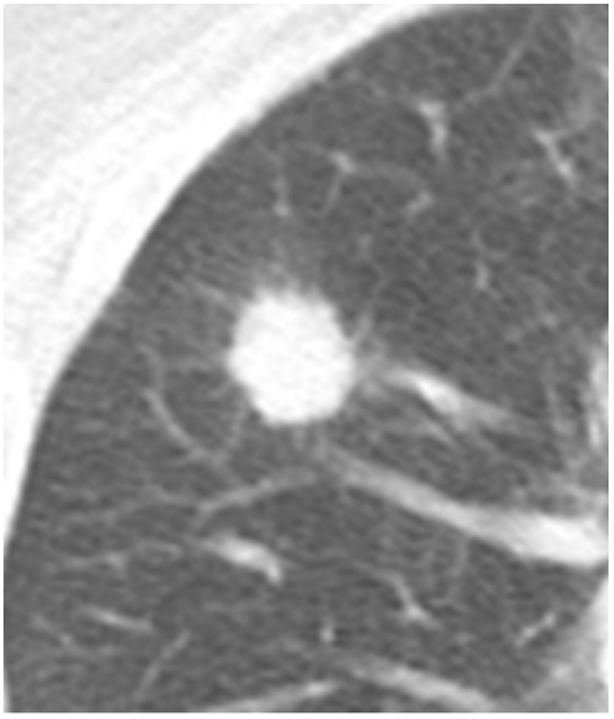

FIGURE 6. SPN with ragged margin suggests a growth pattern along the alveolar wall, as seen in adenocarcinoma with lepidic growth pattern. See Figure 1 legend for expansion of abbreviation.

obscure the lung parenchyma. In distinction, subsolid nodules include both pure GGNs (Fig 17) and partly solid GGNs (Fig 18). GGNs are defined as focal nodular areas of increased lung attenuation through which normal parenchymal structures such as airways, vessels, and interlobular septa are visible.[78] GGNs are frequently multiple and the approach to multiple GGNs is different from solitary GGNs; however, it is out of scope of this article.

As recently characterized by the International Association for the Study of Lung Cancer (IASLC), the American Thoracic Society (ATS), and the European Respiratory Society (ERS), subsolid nodules frequently represent the histologic spectrum of adenocarcinomas, including atypical adenomatous hyperplasia, adenocarcinomas in situ, minimally invasive adenocarcinomas, and lepidic predominant adenocarcinomas (Figs 16A-C, 17).[79] The CT scan patterns recognized in the new IASLC/ATS/ERS lung adenocarcinoma classification are summarized in Table 5.[79]

The presence of more solid components in the GGN on the CT scan is associated with more invasive pathologic features. Despite this correlation, distinguishing benign from malignant subsolid nodules based on radiologic characteristics alone remains problematic, owing to their slower growth rate and correspondingly low metabolic activity. Clinically, this translates to the likelihood of malignancy still being significant even if no growth is demonstrated in a SPN over 2 years or if the ^{18}F-2-deoxy-2-fluoro-D-glucose (FDG)-PET scan fails to demonstrate activity. In a study of lung cancers identified at screening CT imaging, the volume doubling time was higher for this spectrum of adenocarcinomas (988 ± 470 days for atypical adenomatous hyperplasia and 567 ± 168 days for bronchoalveolar carcinoma) compared with squamous cell carcinomas (122 ± 68 days).[80] Tsunezuka et al[81] found that on FDG-PET imaging, the false-negative rate for nodules that would include adenocarcinoma in situ, minimally invasive adenocarcinomas, and lepidic predominant adenocarcinomas in the new IASLC/ATS/ERS adenocarcinomas classification (formerly known as Noguchi lesions of type A, type B, and type C[82]) were 100%, 80%, and 47%, respectively, while the true-positive rate for overtly invasive adenocarcinomas (formerly Noguchi types D, E, and F lesions) was 81.8%. Similar results were reported by Yap et al.[83] Thus, it appears that subsolid nodules may often be malignant and yet demonstrate a doubling time > 2 years or a negative PET scan.

Management of GGNs is controversial at this time. Based on current literature and taking into consideration the aforementioned issues, we have proposed an alternative approach for subsolid nodules, as seen in our diagnostic algorithm. This approach does not differentiate between low- and high-risk groups, as per the original Fleischner criteria,[48] because adenocarcinomas frequently affect younger and nonsmoking patients.

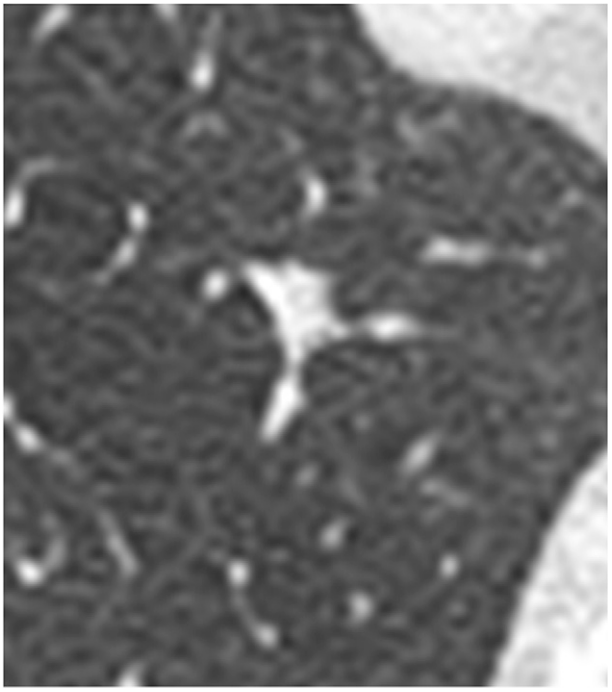

FIGURE 7. SPN with polygonal margins, usually suggestive of a benign etiology. Such a pattern is seen in fibrosis, focal atelectasis, and alveolar infiltration. See Figure 1 legend for expansion of abbreviation.

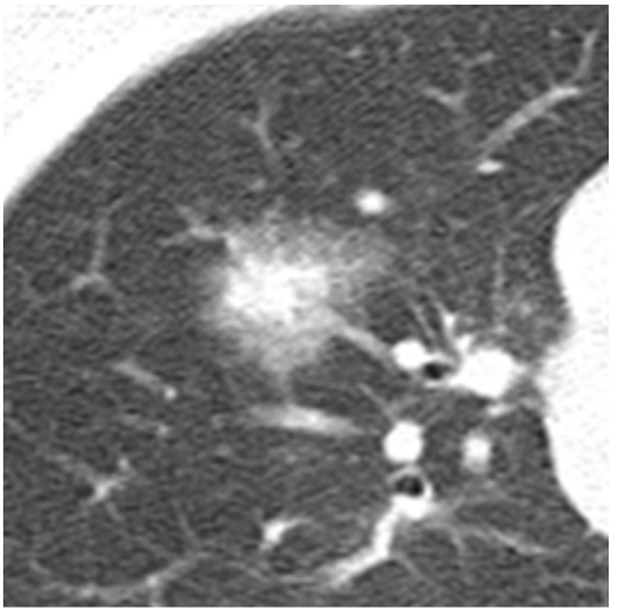

FIGURE 8. SPN with surrounding halo and ground glass attenuation. This is seen in aspergillosis, Kaposi sarcoma, granulomatosis with polyangiitis (Wegener), and metastatic angiosarcoma. Adenocarcinoma can produce a halo due to lepidic growth. See Figure 1 legend for expansion of abbreviation.

Radiographic Characteristics: Combined PET-CT Imaging

Combined PET-CT imaging is a relatively new multimodality technology that allows the correlation of results from two simultaneous and complementary imaging modalities. The CT imaging component demonstrates anatomic detail but does not provide functional information, whereas FDG-PET imaging reveals aspects of tumor function and metabolism. With combined PET-CT imaging, as with CT imaging alone, there are specific characteristics of SPNs on imaging that may help differentiate benign from malignant disease. Malignant cells are more metabolically active and import glucose more avidly than other tissues. This concept forms the basis for PET imaging, which is performed after administration of a glucose analog that has been tagged with a positron-emitting isotope of fluorine, FDG. Whereas the CT image delineates the anatomy of the SPN, the FDG-PET scan, in essence, reveals its pathophysiology. A nodule's metabolic activity is quantified using the standardized uptake value (SUV); a high SUV indicates robust FDG uptake due to high metabolic activity, which suggests malignancy (Fig 19).

Growth Rate

Currently, three-dimensional volumetric measurement of SPNs on CT chest scan provides an accurate assessment of their growth rate when their diameter is >8 mm. It might be suitable to assess changes in tumors by tumor activity, which can be measured by FDG uptake on PET scan, but experience with combined PET-CT imaging in this setting is still limited at this time. Only a few series have assessed the role of combined PET-CT imaging in response to radiotherapy, and there are no data supporting an approach involving serial PET scans to assess nodule size.[84]

Size

PET scans are recommended only for nodules that are >8 to 10 mm in diameter because the sensitivity decreases for the smaller pulmonary nodules. Nodules <1 cm and GGN have a high rate of false-negative interpretation.

SUV Characteristics

The metabolic activity of a nodule is quantified using the SUV; a high SUV indicates increased FDG uptake due to high metabolic activity, which is suggestive of malignancy. A mean SUV value >2.5 is the cutoff at which PET scan has optimal sensitivity and specificity.[85]

Combined PET-CT scan studies can be evaluated in a number of different ways. One method is to measure the SUV level. Another method is to grade the confidence of malignancy by visual analysis. This is done by the nuclear radiologist using a grading system that compares the SUV to the normal FDG uptake

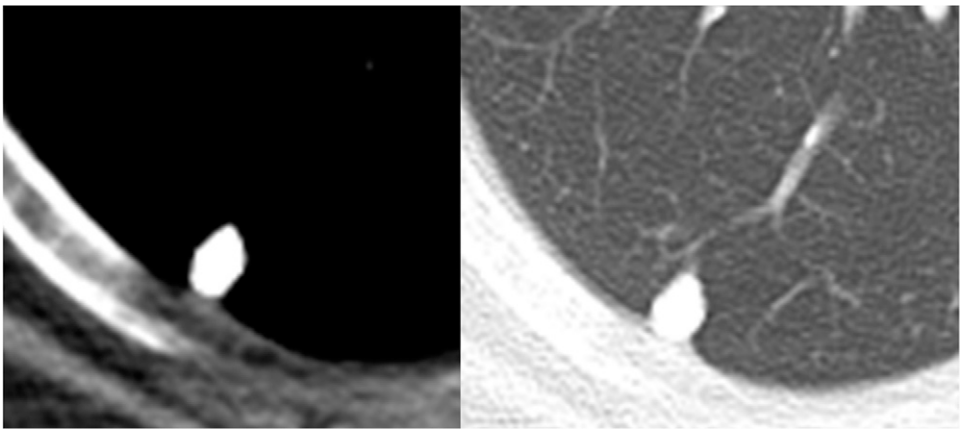

FIGURE 9. SPN with diffuse calcification as seen on (left) mediastinal windows and (right) lung windows, usually suggest benign etiology. See Figure 1 legend for expansion of abbreviation.

within the thorax. Both methods are accepted, but in most cases measuring the SUV does not improve diagnostic accuracy beyond that obtained with simple visual interpretation.[86]

In difficult cases, prolonged observation of the metabolic activity of the nodules has proven to help in the differential diagnosis. There are data that suggest that dual time-point FDG-PET scanning may improve sensitivity and possibly specificity in the evaluation of pulmonary nodules, especially in small- to medium-sized nodules if the nodules retain a higher percentage of their activity at ≥ 2 h.[87] However, this is not currently recommended given the paucity of data and the conflicting findings in different studies.

It should be noted that variations in body habitus, duration of the uptake period, plasma glucose levels, and partial-volume effects can create marked fluctuations in SUV levels. In these situations, combined PET-CT imaging can be falsely positive or negative and this needs to be taken in consideration in complex cases.[88]

Diagnostic Accuracy of Imaging Modalities

Chest Radiographs

The chest radiograph is not recommended as a screening tool for lung cancer, and indeed has a very low sensitivity for detecting SPNs.[39] A significant number of SPNs are missed on chest radiographs, even by experienced radiologists, especially in the upper lobes and peripheral lung zones where they may be obscured by bony structures.[89-93] Moreover, the chest radiograph lacks sufficient resolution to visualize the morphologic characteristics of SPNs discussed previously. If a SPN is visible on chest radiograph, and if a previous radiograph is not available to demonstrate stability over ≥ 2 years, a CT scan of the chest should be performed with thin sections through the nodule to better delineate its morphology.

CT Scan

The CT scan is more sensitive than the chest radiograph in detecting SPNs, as it eliminates superimposition

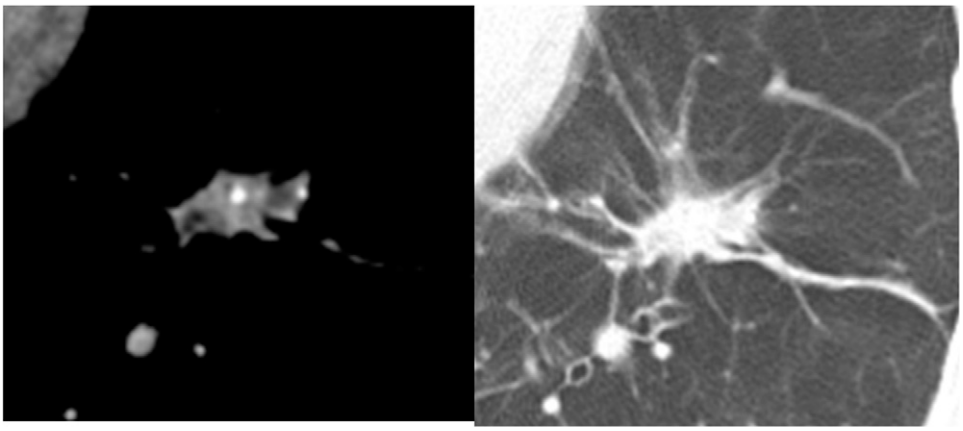

FIGURE 10. SPN with central calcification usually suggestive of a benign etiology. It should be noted that it is quite uncommon to come across a truly central calcified nodule. See Figure 1 legend for expansion of abbreviation.

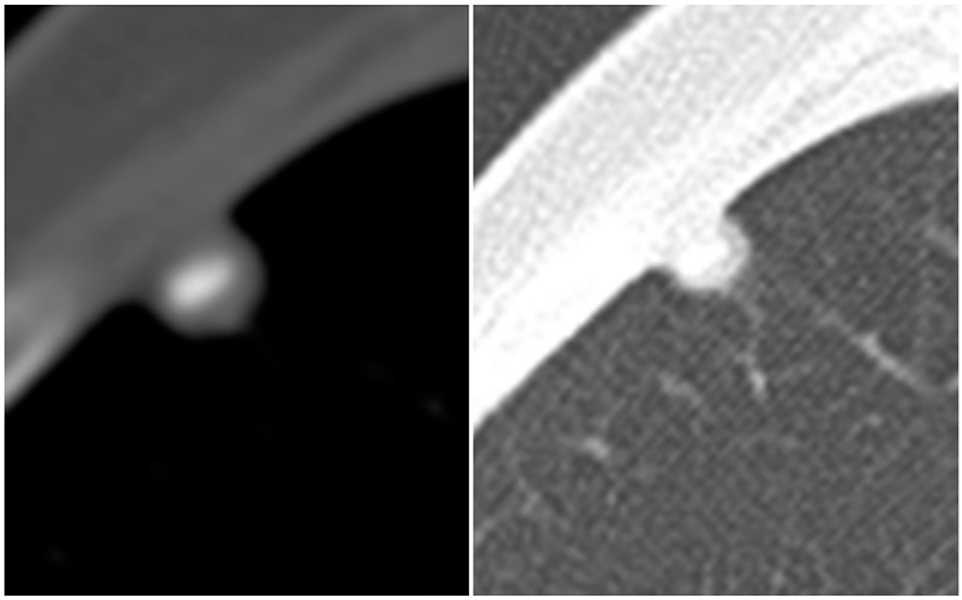

FIGURE 11. SPN with laminated calcification, usually suggestive of a benign etiology. See Figure 1 legend for expansion of abbreviation.

of structures. The SPN, once visualized on CT scan, can provide clues as to its nature, that is, benign vs malignant, based on the morphologic characteristics discussed previously in this article.[39] Initially, there was enthusiasm about CT imaging with dynamic contrast enhancement, but with the advent of PET scan it has been marginalized.

In patients with a CT scan-based evaluation of a likely malignant, solid SPN (clinical T1N0M0 or stage I lung cancer), 5% to 21% patients are still found to have positive lymph node involvement during surgical sampling.[94-98] This suggests that an important clue to the benign vs malignant nature of a SPN, that is, involvement of hilar and mediastinal lymph nodes, is missed quite often on CT scan. Indeed, meta-analyses on the accuracy of CT scanning for staging the mediastinum in patients with lung cancer have revealed a sensitivity of only 51% to 64% and a specificity of 74% to 86%.[99-101] Studies specifically looking at stage T1 lung cancer have found even lower sensitivity: 27% to 41%.[96,102] CT imaging of the chest also does not take into account the possibility of distant metastases from a malignant SPN, which, albeit infrequent, should nevertheless not be ignored.[103] Some centers have studied the utility of lack of contrast enhancement of a nodule to point toward a benign etiology. However, as will be mentioned in the next section of this article, combined PET-CT scans, by shedding

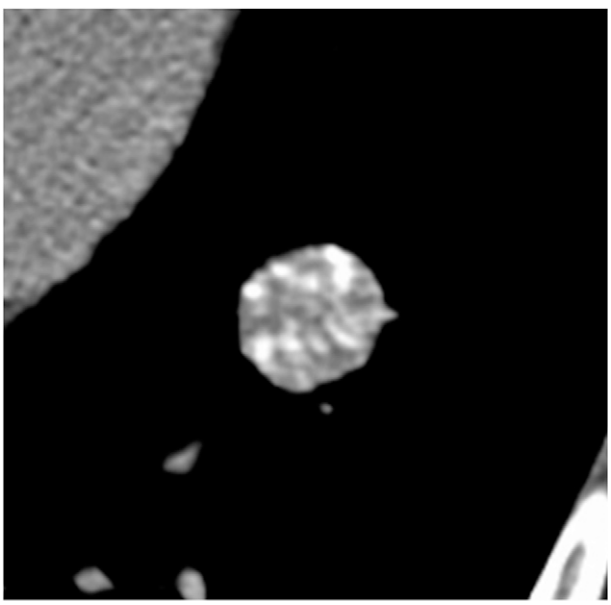

FIGURE 12. SPN with popcorn calcification. It is suggestive of a benign etiology such as hamartoma. See Figure 1 legend for expansion of abbreviation.

Table 4—*Patterns of Calcification in SPNs*

Pattern of Calcification	Etiology
Laminated and concentric	Usually benign
Dense central core	Usually benign
Diffuse and solid	Usually benign
Popcorn	Hamartoma
Punctate	Malignant lesions: scar carcinoma, typical and atypical carcinoids, large-cell neuroendocrine carcinoma and metastasis from colon, ovary, breast, thyroid, and osteogenic tumors.[58,59]
Eccentric	Due to necrosis within the malignant nodule or engulfment of adjacent granuloma[40,60-62]

See Table 2 legend for expansion of abbreviation.

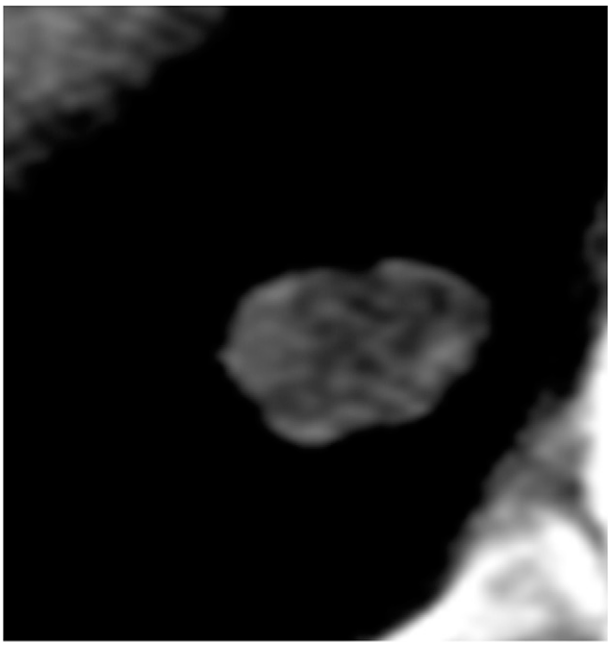

FIGURE 13. An attenuation value between −40 and −120 Hounsfield units suggests presence of fat in a SPN. Fat is present in up to 60% of hamartomas. See Figure 3 legend for expansion of abbreviation.

FIGURE 14. SPN with cavitation is seen in necrotic malignant SPNs such as squamous cell carcinoma. It may also be seen in benign SPNs such as abscesses, infectious granulomas, vasculitides, lymphoid interstitial pneumonia, early Langerhans-cell histiocytosis, and pulmonary infarction. See Figure 1 legend for expansion of abbreviation.

light on both anatomic and functional characteristics of the nodule, have replaced CT scan with contrast enhancement for this purpose. It should be pointed out that in November 2010, the National Lung Cancer Screening Trial reported 20% fewer lung cancer deaths among trial participants screened with low-dose helical CT scan compared with those who were screened with chest radiographs. It is, therefore, very likely that more SPNs will be detected in the future, thus escalating the importance of clinical and radiographic guidelines for its management.[104]

FDG-PET/Combined PET-CT Scanning

FDG-PET scanning is very accurate in differentiating benign from malignant lesions in nodules as small as 1 cm. A meta-analysis of 12 studies with 624 patients demonstrated a sensitivity of 96%, specificity of 79%, and accuracy of 91%.[105] Gould et al[106] reported a sensitivity of 94.2% and specificity of 83.3% in a meta-analysis of 13 studies evaluating 450 patients with nodules >8-10 mm. Another review of 17 studies revealed a sensitivity of 80% to 100% and specificity of 40% to 100%; pooled sensitivity and specificity values were 87% and 83%, respectively, for nodules measuring >8-10 mm.[90] In a subsequent prospective study of 344 participants, the sensitivities of PET and CT imaging to aid detection of a malignant nodule were found to be similar (91.7% vs 95.6%), but the specificity of PET scans was superior to CT scans (82.3% vs 40.6%). In this study, PET scan was also found to have superior interobserver and intraobserver reliability, compared with CT imaging. The average nodule size in this study was 16 mm.[107]

In a retrospective study of 100 patients, 40 of whom had malignant SPNs, the sensitivity values for CT, PET, and integrated PET-CT scans were 82%, 88%, and 88%, respectively, whereas the specificity values were 66%, 71%, and 77%, respectively.[108] PET-CT imaging provided significantly better specificity than CT scan alone or PET scan alone, and had a positive predictive value (PPV) of 72% and a negative predictive value (NPV) of 90%. The higher specificity of PET-CT imaging was attributed to the ability to discard false-positive PET scan uptake on the basis of CT scan morphology showing benign patterns of calcification. Another retrospective analysis of 119 patients, 79 of whom had malignant SPNs, yielded sensitivity, specificity, and accuracy of 96%, 88%, and 93%, respectively, with integrated PET-CT imaging; this accuracy was higher than contrast-enhanced CT scan. The NPV of PET-CT scanning was 92%, leading the authors to conclude that a SPN with a negative PET-CT scan could safely be followed up over time.[109] Several other studies have yielded similarly high sensitivity and accuracy for integrated PET-CT scanning.[110-112] Interestingly, these studies found that visual analysis of SUV yields better accuracy than semiquantitative analysis; in other words, considering any uptake on PET scanning as malignant yields better sensitivity than considering a particular SUV cutoff.

FIGURE 15. SPN with bubbly lucencies. Bubbly lucencies can be seen in adenocarcinoma in situ (previously known as bronchoalveolar carcinoma), pulmonary lymphoma, sarcoidosis, round pneumonia, and organizing pneumonia. See Figure 1 legend for expansion of abbreviation.

In addition to its accuracy in determining the benign vs malignant nature of a SPN, combined FDG-PET scanning provides additional clues in the form of an evaluation of the mediastinal lymph nodes for possible metastases. In a meta-analysis of 44 studies with 2,865 patients with lung cancer, the sensitivity and specificity for identifying mediastinal metastases with PET scans were 74% and 85%, respectively, which is more accurate than CT scanning.[99] In a retrospective study of 184 patients with clinical stage T1 non-small cell lung cancer (NSCLC), pathologic N2 disease was identified in 23 (12%) patients. PET-CT scanning had an N2-disease detection sensitivity of 48%, specificity of 95%, and accuracy of 89%.[113] In another prospective study of 150 patients with clinical stage T1 NSCLC, the sensitivity, specificity, PPV, NPV, and accuracy of combined PET-CT scanning in detecting mediastinal nodal involvement were 47%, 100%, 100%, 87%, and 88%, respectively.[114] The low sensitivity of combined PET-CT scans in stage T1 NSCLC is likely attributed to its inability to detect early-stage or microscopic metastases. Although more studies are needed to assess the role of combined PET-CT scanning in stage T1 NSCLC, that is, malignant SPNs, it appears that the high specificity and accuracy can be used to an advantage while evaluating SPNs. The lack of mediastinal uptake should not rule out the possibility of malignancy, but the presence of uptake should serve as a clue that malignancy is a possibility.

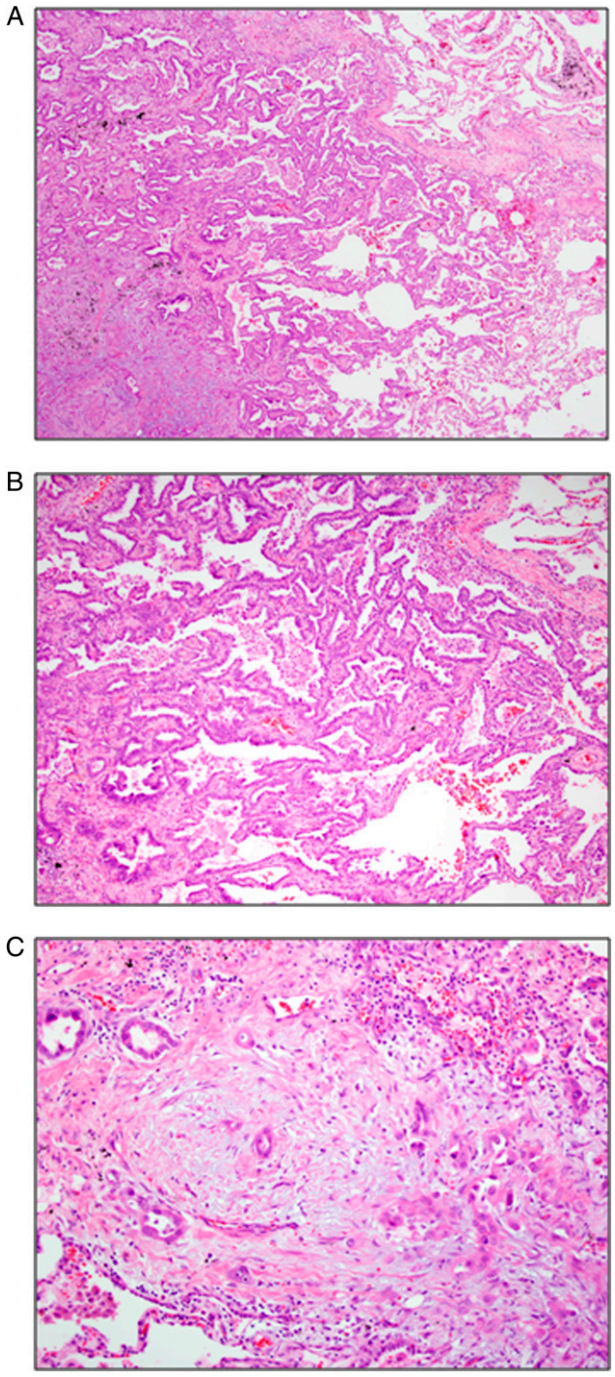

FIGURE 16. A, Lepidic predominant adenocarcinoma with lepidic component and acinar component. B, Lepidic predominant adenocarcinoma. Most of the image shows lepidic adenocarcinoma with small foci of invasive acinar adenocarcinoma. C, This pattern of invasive acinar adenocarcinoma shows a desmoplastic stromal response.

It is important to understand the shortcomings of PET scanning. The sensitivity of detecting SPNs <8 to 10 mm in diameter is low, likely because the mass of metabolically active cells is too small to be detected with the aid of PET scanning, so its use in such nodules should be avoided.[115] Tumors that have low metabolic activity (eg, adenocarcinomas in situ, carcinoids) can

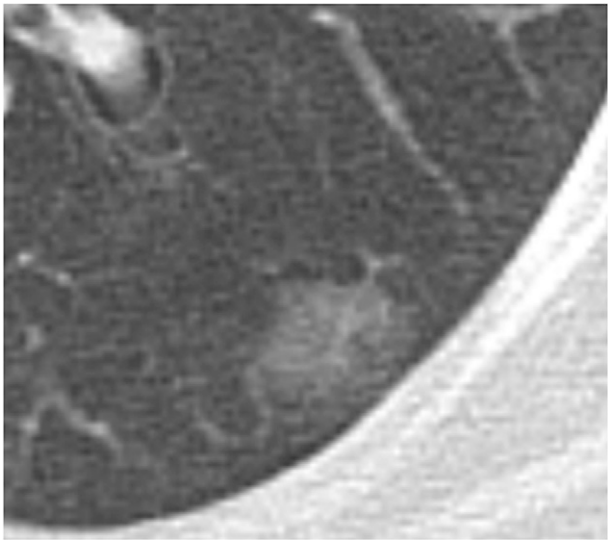

FIGURE 17. Ground glass opacity (GGO) in a SPN. GGOs are defined as focal nodular areas of increased lung attenuation through which normal parenchymal structures such as airways, vessels, and interlobular septa are visible. See Figure 1 legend for expansion of other abbreviation.

yield false-negative results, as discussed previously. Finally, a significant number of false-negative results have been found in high-risk patient populations, notably SPNs detected during screening studies.[116-118] Although nodules < 1 cm and GGN accounted for a fair share of the false-negatives, it nevertheless appears that FDG-PET imaging is most suited to evaluating SPNs with intermediate pretest probability of malignancy. Patients with a high pretest probability should proceed to a surgical biopsy procedure even if an FDG-PET scan is negative. Interestingly,

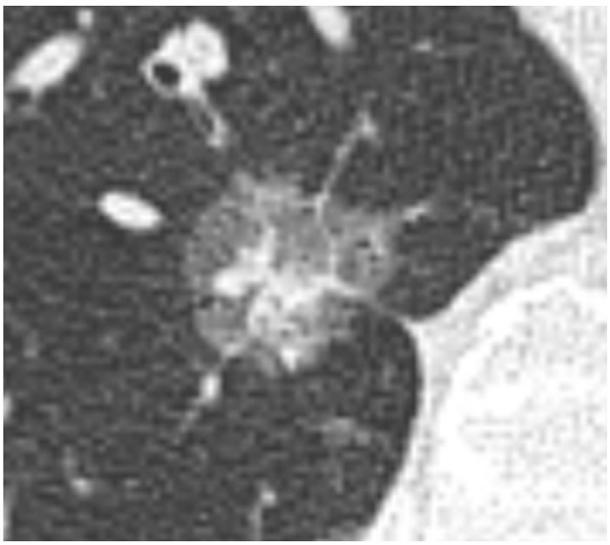

FIGURE 18. A partly solid SPN. See Figure 1 legend for expansion of abbreviation.

Table 5—*CT Patterns Among IASLC/ATS/ERS Lung Adenocarcinoma Subtypes*

Predominant Histologic Subtype	Appearance on CT Scan
Nonmucinous AIS MIA	Most often pure GGN or partly solid nodule with solid component < 5 mm
Lepidic (nonmucinous)	Most often partly solid nodule with solid component > 5 mm or solid nodule; less commonly pure GGN
Papillary	Solid nodule
Acinar	Solid nodule
Micropapillary	Unknown
Solid	Solid
Invasive mucinous adenocarcinoma	Consolidation, air bronchograms; less often pure GGN

AIS = adenocarcinoma in situ; ATS = American Thoracic Society; ERS = European Respiratory Society; GGN = ground glass nodule; IASLC = International Association for the Study of Lung Cancer; MIA = minimally invasive adenocarcinoma.

patients with malignant SPNs and false-negative FDG-PET scan results may have a favorable prognosis even when curative intent surgery is delayed by up to 238 days.[119,120] Therefore, patients with negative findings on FDG-PET scan should still be followed up with serial imaging for at least 2 years to confirm a benign diagnosis. False-positive results are also well described, not only for the SPN but for the mediastinum: Infectious and inflammatory conditions such as TB, endemic mycoses, sarcoidosis, and others can yield false-positive results. Tissue biopsy specimens therefore remain the gold standard in elucidating the final diagnosis of the SPN. The advantages and disadvantages of PET scanning are tabulated in Table 6.

Paradoxically, in subsolid nodules, FDG-PET scan can reveal higher SUV in inflammatory nodules compared with malignant nodules, as shown in a study by Chun et al.[121] Similarly, Tsushima et al[122] found that SUV > 1.5 is suggestive of a benign etiology in SPN with subsolid components on FDG-PET scan. Given this paradox, FDG-PET imaging cannot be reliably used to differentiate benign vs malignant subsolid SPN. In addition, there is a low incidence of nodal and distant metastasis in subsolid nodules, which lowers FDG-PET scan sensitivity.[123]

MRI

New literature is emerging regarding the use of dynamic MRI to distinguish benign from malignant SPN. Dynamic MRI values have been found to reflect the quantitative and morphologic characteristics of microvessels in SPNs, similar in concept to dynamic CT imaging.[124] In a study of 202 SPNs,[125] dynamic MR images were obtained before and up to 8 min after IV injection of gadopentetate dimeglumine using

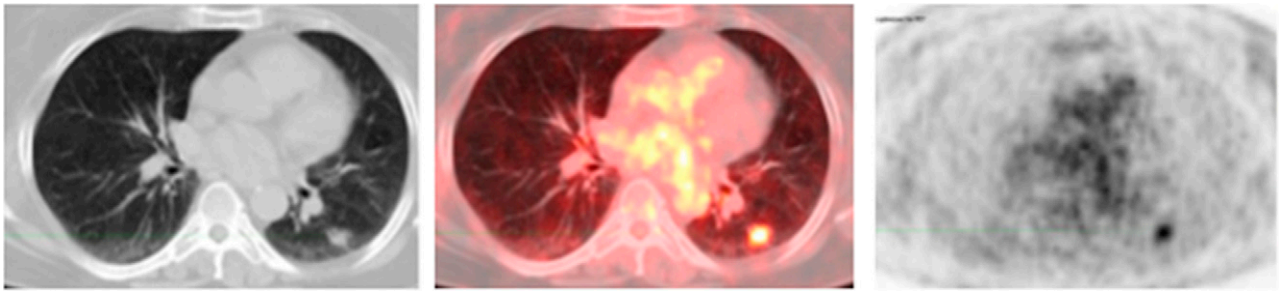

FIGURE 19. Combined PET-CT scan showing ^{18}F-2-deoxy-2-fluoro-D-glucose-avid SPN. Malignant cells are more metabolically active and import glucose more avidly than other tissues. See Figure 1 legend for expansion of abbreviation.

T1-weighted spin-echo sequences. With ≤110% maximum enhancement ratio as a cutoff value, the PPV for malignancy was 92%; sensitivity, 63%; and specificity, 74%. With ≥13.5%/min slope as a cutoff value, sensitivity, specificity, PPV, and NPV for malignancy were 94%, 96%, 99%, and 74%, respectively. A prospective study of 175 patients with 202 SPNs[126] was recently performed comparing dynamic MRI, dynamic CT imaging, and PET-CT imaging to distinguish benign from malignant SPNs. On dynamic MRI, with a slope of enhancement ratio cutoff of 0.04/s, the sensitivity, specificity, PPV, NPV, and accuracy were 96.3%, 82.1%, 95.7%, 84.2%, and 93.6%, respectively. These results were superior to combined PET-CT and dynamic CT imaging, and have opened up a promising new avenue of research in the use of imaging modalities to characterize SPNs.

CONCLUSION

Morphologic characteristics of SPN can help distinguish benign from malignant SPNs. These features include volume doubling time, size, margins, presence and nature of calcification, presence of fat, and wall thickness in case of cavitation. GGNs, while usually multiple, are further classified as pure ground glass and partly solid. Thin-section CT scans allow accurate delineation of these morphologic features. In conjunction, FDG-PET scans provide a window to the metabolic activity of the nodules, giving valuable pathophysiologic information about them.

Table 6—*Advantages and Disadvantages of FDG-PET Imaging*

Advantages	Disadvantages
Accurate noninvasive evaluation	Lower sensitivity for lesions < 8 mm
Whole-body image detects extrapulmonary tumors	False positives from inflammation
Ability to stage known lung cancer	False negatives from tumors with low metabolic rate

FDG = ^{18}F-2-deoxy-2-fluoro-D-glucose.

ACKNOWLEDGMENTS

Financial/nonfinancial disclosures: The authors have reported to *CHEST* that no potential conflicts of interest exist with any companies/organizations whose products or services may be discussed in this article.

Other contributions: The authors wish to thank Patrice Balistreri, administrative assistant, for her invaluable clerical assistance.

REFERENCES

1. Tuddenham WJ. Glossary of terms for thoracic radiology: recommendations of the Nomenclature Committee of the Fleischner Society. *AJR Am J Roentgenol*. 1984;143(3):509-517.
2. Shiau MC, Portnoy E, Garay SM. Management of solitary pulmonary nodules. In: Kanne JP, ed. *Clinically Oriented Pulmonary Imaging*. New York, NY: Springer; 2012:19-27.
3. Holin SM, Dwork RE, Glaser S, Rikli AE, Stocklen JB. Solitary pulmonary nodules found in a community-wide chest roentgenographic survey; a five-year follow-up study. *Am Rev Tuberc*. 1959;79(4):427-439.
4. Swensen SJ, Silverstein MD, Edell ES, et al. Solitary pulmonary nodules: clinical prediction model versus physicians. *Mayo Clin Proc*. 1999;74(4):319-329.
5. Henschke CI, McCauley DI, Yankelevitz DF, et al. Early Lung Cancer Action Project: overall design and findings from baseline screening. *Lancet*. 1999;354(9173):99-105.
6. Veronesi G, Bellomi M, Spaggiari L, et al. Low dose spiral computed tomography for early diagnosis of lung cancer. Results of baseline screening in 5,000 high-risk volunteers. *J Clin Oncol*. 2006;24(18S):7029.
7. Henschke CI, Yankelevitz DF, Naidich DP, et al. CT screening for lung cancer: suspiciousness of nodules according to size on baseline scans. *Radiology*. 2004;231(1):164-168.
8. Gohagan J, Marcus P, Fagerstrom R, Pinsky P, Kramer B, Prorok P; Writing Committee, Lung Screening Study Research Group. Baseline findings of a randomized feasibility trial of lung cancer screening with spiral CT scan vs chest radiograph: the Lung Screening Study of the National Cancer Institute. *Chest*. 2004;126(1):114-121.
9. Li F, Sone S, Abe H, Macmahon H, Doi K. Malignant versus benign nodules at CT screening for lung cancer: comparison of thin-section CT findings. *Radiology*. 2004;233(3):793-798.
10. Swensen SJ, Jett JR, Hartman TE, et al. Lung cancer screening with CT: Mayo Clinic experience. *Radiology*. 2003;226(3):756-761.
11. Nawa T, Nakagawa T, Kusano S, Kawasaki Y, Sugawara Y, Nakata H. Lung cancer screening using low-dose spiral CT: results of baseline and 1-year follow-up studies. *Chest*. 2002;122(1):15-20.

12. Henschke CI, Yankelevitz DF, Libby DM, et al. Early lung cancer action project: annual screening using single-slice helical CT. *Ann N Y Acad Sci*. 2001;952:124-134.
13. Diederich S, Wormanns D, Lenzen H, Semik M, Thomas M, Peters PE. Screening for asymptomatic early bronchogenic carcinoma with low dose CT of the chest. *Cancer*. 2000; 89(suppl 11):2483-2484.
14. Wahidi MM, Govert JA, Goudar RK. Evidence for the treatment of patients with pulmonary nodules: when is it lung cancer?: ACCP evidence-based clinical practice guidelines (2nd edition). *Chest*. 2007;132(suppl 3):94S-107S.
15. Patel VK, Naik SK, Naidich DP, et al. A practical algorithmic approach to the diagnosis of solitary pulmonary nodules: part 2: pretest probability and algorithm. *Chest*. 2013; 143(3):840-846.
16. Gurney JW. Determining the likelihood of malignancy in solitary pulmonary nodules with Bayesian analysis. Part I. Theory. *Radiology*. 1993;186(2):405-413.
17. Swensen SJ, Silverstein MD, Ilstrup DM, Schleck CD, Edell ES. The probability of malignancy in solitary pulmonary nodules. Application to small radiologically indeterminate nodules. *Arch Intern Med*. 1997;157(8):849-855.
18. Gould MK, Ananth L, Barnett PG; Veterans Affairs SNAP Cooperative Study Group. A clinical model to estimate the pretest probability of lung cancer in patients with solitary pulmonary nodules. *Chest*. 2007;131(2):383-388.
19. Peto R, Lopez AD, Boreham J. *Mortality From Smoking in Developed Countries 1950-2000. Indirect Estimates From National Vital Statistics*. Oxford, England: Oxford University Press; 1994.
20. Quint LE, Park CH, Iannettoni MD. Solitary pulmonary nodules in patients with extrapulmonary neoplasms. *Radiology*. 2000;217(1):257-261.
21. Sortini A, Carcoforo P, Ascanelli S, Sortini D, Pozza E. Significance of a single pulmonary nodule in patients with previous history of malignancy. *Eur J Cardiothorac Surg*. 2001;20(6):1101-1105.
22. Mery CM, Pappas AN, Bueno R, et al. Relationship between a history of antecedent cancer and the probability of malignancy for a solitary pulmonary nodule. *Chest*. 2004;125(6): 2175-2181.
23. Bouros D, Hatzakis K, Labrakis H, Zeibecoglou K. Association of malignancy with diseases causing interstitial pulmonary changes. *Chest*. 2002;121(4):1278-1289.
24. Kawai T, Yakumaru K, Suzuki M, Kageyama K. Diffuse interstitial pulmonary fibrosis and lung cancer. *Acta Pathol Jpn*. 1987;37(1):11-19.
25. Nagai A, Chiyotani A, Nakadate T, Konno K. Lung cancer in patients with idiopathic pulmonary fibrosis. *Tohoku J Exp Med*. 1992;167(3):231-237.
26. Aubry ME, Myers JL, Douglas WW. Primary pulmonary carcinomas in patients with idiopathic pulmonary fibrosis. *Mayo Clin Proc*. 2002;77(8):77.
27. Kawasaki H, Nagai K, Yokose T, et al. Clinicopathological characteristics of surgically resected lung cancer associated with idiopathic pulmonary fibrosis. *J Surg Oncol*. 2001;76(1): 53-57.
28. Turner-Warwick M, Lebowitz M, Burrows B, Johnson A. Cryptogenic fibrosing alveolitis and lung cancer. *Thorax*. 1980;35(7):496-499.
29. Kishi K, Homma S, Kurosaki A, Motoi N, Yoshimura K. High-resolution computed tomography findings of lung cancer associated with idiopathic pulmonary fibrosis. *J Comput Assist Tomogr*. 2006;30(1):95-99.
30. Kim KI, Leung AN, Flint JD, Müller NL. Chronic pulmonary coccidioidomycosis: computed tomographic and pathologic findings in 18 patients. *Can Assoc Radiol J*. 1998;49(6):401-407.
31. Lindell RM, Hartman TE, Nadrous HF, Ryu JH. Pulmonary cryptococcosis: CT findings in immunocompetent patients. *Radiology*. 2005;236(1):326-331.
32. Fox DL, Müller NL. Pulmonary cryptococcosis in immunocompetent patients: CT findings in 12 patients. *AJR Am J Roentgenol*. 2005;185(3):622-626.
33. Murayama S, Sakai S, Soeda H, et al. Pulmonary cryptococcosis in immunocompetent patients: HRCT characteristics. *Clin Imaging*. 2004;28(3):191-195.
34. Nathan MH, Collins VP, Adams RA. Differentiation of benign and malignant pulmonary nodules by growth rate. *Radiology*. 1962;79:221-232.
35. Garland LH, Coulson W, Wollin E. The rate of growth and apparent duration of untreated primary bronchial carcinoma. *Cancer*. 1963;16:694-707.
36. Steele JD, Buell P. Asymptomatic solitary pulmonary nodules. Host survival, tumor size, and growth rate. *J Thorac Cardiovasc Surg*. 1973;65(1):140-151.
37. Weiss W. Tumor doubling time and survival of men with bronchogenic carcinoma. *Chest*. 1974;65(1):3-8.
38. Friberg S, Mattson S. On the growth rates of human malignant tumors: implications for medical decision making. *J Surg Oncol*. 1997;65(4):284-297.
39. Bach PB, Silvestri GA, Hanger M. Screening for lung cancer: ACCP evidence-based clinical practice guidelines (2nd edition). *Chest*. 2007;132(suppl 3):69S-77S.
40. Soubani AO. The evaluation and management of the solitary pulmonary nodule. *Postgrad Med J*. 2008;84(995):459-466.
41. Nietert PJ, Ravenel JG, Leue WM, et al. Imprecision in automated volume measurements of pulmonary nodules and its effect on the level of uncertainty in volume doubling time estimation. *Chest*. 2009;135(6):1580-1587.
42. Yankelevitz DF, Henschke CI. Small solitary pulmonary nodules. *Radiol Clin North Am*. 2000;38(3):471-478.
43. Erasmus JJ, McAdams HP, Connolly JE. Solitary pulmonary nodules: part II. Evaluation of the indeterminate nodule. *Radiographics*. 2000;20(1):59-66.
44. Revel MP, Merlin A, Peyrard S, et al. Software volumetric evaluation of doubling times for differentiating benign versus malignant pulmonary nodules. *AJR Am J Roentgenol*. 2006;187(1):135-142.
45. Park CM, Goo JM, Lee HJ, Kim KG, Kang MJ, Shin YH. Persistent pure ground-glass nodules in the lung: interscan variability of semiautomated volume and attenuation measurements. *AJR Am J Roentgenol*. 2010;195(6):W408-W414.
46. Singh S, Pinsky P, Fineberg NS, et al. Evaluation of reader variability in the interpretation of follow-up CT scans at lung cancer screening. *Radiology*. 2011;259(1):263-270.
47. Zerhouni EA, Stitik FP, Siegelman SS, et al. CT of the pulmonary nodule: a cooperative study. *Radiology*. 1986; 160(2):319-327.
48. MacMahon H, Austin JH, Gamsu G, et al; Fleischner Society. Guidelines for management of small pulmonary nodules detected on CT scans: a statement from the Fleischner Society. *Radiology*. 2005;237(2):395-400.
49. Swensen SJ, Viggiano RW, Midthun DE, et al. Lung nodule enhancement at CT: multicenter study. *Radiology*. 2000; 214(1):73-80.
50. Winer-Muram HT. The solitary pulmonary nodule. *Radiology*. 2006;239(1):34-49.
51. Furuya K, Murayama S, Soeda H, et al. New classification of small pulmonary nodules by margin characteristics on high-resolution CT. *Acta Radiol*. 1999;40(5):496-504.
52. Seemann MD, Seemann O, Luboldt W, et al. Differentiation of malignant from benign solitary pulmonary lesions using chest radiography, spiral CT and HRCT. *Lung Cancer*. 2000;29(2):105-124.

53. Zwirewich CV, Vedal S, Miller RR, Müller NL. Solitary pulmonary nodule: high-resolution CT and radiologic-pathologic correlation. *Radiology*. 1991;179(2):469-476.
54. Siegelman SS, Zerhouni EA, Leo FP, Khouri NF, Stitik FP. CT of the solitary pulmonary nodule. *AJR Am J Roentgenol*. 1980;135(1):1-13.
55. Khan A, Herman PG, Vorwerk P, Stevens P, Rojas KA, Graver M. Solitary pulmonary nodules: comparison of classification with standard, thin-section, and reference phantom CT. *Radiology*. 1991;179(2):477-481.
56. Huston J III, Muhm JR. Solitary pulmonary opacities: plain tomography. *Radiology*. 1987;163(2):481-485.
57. Kuhlman JE, Fishman EK, Siegelman SS. Invasive pulmonary aspergillosis in acute leukemia: characteristic findings on CT, the CT halo sign, and the role of CT in early diagnosis. *Radiology*. 1985;157(3):611-614.
58. Primack SL, Hartman TE, Lee KS, Müller NL. Pulmonary nodules and the CT halo sign. *Radiology*. 1994;190(2): 513-515.
59. Ikehara M, Saito H, Kondo T, et al. Comparison of thin-section CT and pathological findings in small solid-density type pulmonary adenocarcinoma: prognostic factors from CT findings. *Eur J Radiol*. 2012;81(1):189-194.
60. Yankelevitz DF, Henschke CI. Derivation for relating calcification and size in small pulmonary nodules. *Clin Imaging*. 1998;22(1):1-6.
61. Takamochi K, Yokose T, Yoshida J, et al. Calcification in large cell neuroendocrine carcinoma of the lung. *Jpn J Clin Oncol*. 2003;33(1):10-13.
62. Cardinale L, Ardissone F, Novello S, et al. The pulmonary nodule: clinical and radiological characteristics affecting a diagnosis of malignancy. *Radiol Med (Torino)*. 2009:114(6): 871-879.
63. Mahoney MC Sr, Shipley RT, Corcoran HL, Dickson BA. CT demonstration of calcification in carcinoma of the lung. *AJR Am J Roentgenol*. 1990;154(2):255-258.
64. Stewart JG, MacMahon H, Vyborny CJ, Pollak ER. Dystrophic calcification in carcinoma of the lung: demonstration by CT. *AJR Am J Roentgenol*. 1987;148(1):29-30.
65. Grewal RG, Austin JH. CT demonstration of calcification in carcinoma of the lung. *J Comput Assist Tomogr*. 1994; 18(6):867-871.
66. Mazzone PJ, Stoller JK. The pulmonologist's perspective regarding the solitary pulmonary nodule. *Semin Thorac Cardiovasc Surg*. 2002;14(3):250-260.
67. Trotman-Dickenson B, Baumert B. Multidetector-row CT of the solitary pulmonary nodule. *Semin Roentgenol*. 2003; 38(2):158-167.
68. McLoud TC, Swenson SJ. Lung carcinoma. *Clin Chest Med*. 1999;20(4):697-713.
69. Siegelman SS, Khouri NF, Scott WW Jr, et al. Pulmonary hamartoma: CT findings. *Radiology*. 1986;160(2):313-317.
70. Klein JS, Braff S. Imaging evaluation of the solitary pulmonary nodule. *Clin Chest Med*. 2008;29(1):15-38.
71. Muram TM, Aisen A. Fatty metastatic lesions in 2 patients with renal clear-cell carcinoma. *J Comput Assist Tomogr*. 2003;27(6):869-870.
72. Woodring JH, Fried AM, Chuang VP. Solitary cavities of the lung: diagnostic implications of cavity wall thickness. *AJR Am J Roentgenol*. 1980;135(6):1269-1271.
73. Woodring JH, Fried AM. Significance of wall thickness in solitary cavities of the lung: a follow-up study. *AJR Am J Roentgenol*. 1983;140(3):473-474.
74. Mirtcheva RM, Vazquez M, Yankelevitz DF, Henschke CI. Bronchioloalveolar carcinoma and adenocarcinoma with bronchioloalveolar features presenting as ground-glass opacities on CT. *Clin Imaging*. 2002;26(2):95-100.
75. Saito H, Yamada K, Hamanaka N, et al. Initial findings and progression of lung adenocarcinoma on serial computed tomography scans. *J Comput Assist Tomogr*. 2009;33(1): 42-48.
76. Kui M, Templeton PA, White CS, Cai ZL, Bai YX, Cai YQ. Evaluation of the air bronchogram sign on CT in solitary pulmonary lesions. *J Comput Assist Tomogr*. 1996;20(6):983-986.
77. Kuriyama K, Tateishi R, Doi O, et al. Prevalence of air bronchograms in small peripheral carcinomas of the lung on thin-section CT: comparison with benign tumors. *AJR Am J Roentgenol*. 1991;156(5):921-924.
78. Godoy MC, Naidich DP. Subsolid pulmonary nodules and the spectrum of peripheral adenocarcinomas of the lung: recommended interim guidelines for assessment and management. *Radiology*. 2009;253(3):606-622.
79. Travis WD, Brambilla E, Noguchi M, et al. International Association for the Study of Lung Cancer/American Thoracic Society/European Respiratory Society international multidisciplinary classification of lung adenocarcinoma. *J Thorac Oncol*. 2011;6(2):244-285.
80. Takashima S, Sone S, Li F, Maruyama Y, Hasegawa M, Kadoya M. Indeterminate solitary pulmonary nodules revealed at population-based CT screening of the lung: using first follow-up diagnostic CT to differentiate benign and malignant lesions. *AJR Am J Roentgenol*. 2003;180(5):1255-1263.
81. Tsunezuka Y, Shimizu Y, Tanaka N, Takayanagi T, Kawano M. Positron emission tomography in relation to Noguchi's classification for diagnosis of peripheral non-small-cell lung cancer 2 cm or less in size. *World J Surg*. 2007;31(2):314-317.
82. Noguchi M, Morikawa A, Kawasaki M, et al. Small adenocarcinoma of the lung. Histologic characteristics and prognosis. *Cancer*. 1995;75(12):2844-2852.
83. Yap CS, Schiepers C, Fishbein MC, Phelps ME, Czernin J. FDG-PET imaging in lung cancer: how sensitive is it for bronchioloalveolar carcinoma? *Eur J Nucl Med Mol Imaging*. 2002;29(9):1166-1173.
84. Ichiya Y, Kuwabara Y, Sasaki M, et al. A clinical evaluation of FDG-PET to assess the response in radiation therapy for bronchogenic carcinoma. *Ann Nucl Med*. 1996;10(2): 193-200.
85. Lowe VJ, Fletcher JW, Gobar L, et al. Prospective investigation of positron emission tomography in lung nodules. *J Clin Oncol*. 1998;16(3):1075-1084.
86. Lowe VJ, Hoffman JM, DeLong DM, Patz EF, Coleman RE. Semiquantitative and visual analysis of FDG-PET images in pulmonary abnormalities. *J Nucl Med*. 1994;35(11):1771-1776.
87. Matthies A, Hickeson M, Cuchiara A, Alavi A. Dual time point 18F-FDG PET for the evaluation of pulmonary nodules. *J Nucl Med*. 2002;43(7):871-875.
88. Keyes JW Jr. SUV: standard uptake or silly useless value? *J Nucl Med*. 1995;36(10):1836-1839.
89. Ketai L, Malby M, Jordan K, Meholic A, Locken J. Small nodules detected on chest radiography: does size predict calcification? *Chest*. 2000;118(3):610-614.
90. Gould M, Fletcher J, Iannettonin M. Evaluation of patients with pulmonary nodules: When is it lung cancer?: ACCP evidence-based clinical practice guidelines (2nd edition). *Chest*. 2007;132(suppl 3):108S-130S.
91. Muhm JR, Miller WE, Fontana RS, Sanderson DR, Uhlenhopp MA. Lung cancer detected during a screening program using four-month chest radiographs. *Radiology*. 1983;148(3):609-615.
92. Quekel LG, Kessels AG, Goei R, van Engelshoven JM. Miss rate of lung cancer on the chest radiograph in clinical practice. *Chest*. 1999;115(3):720-724.
93. Shah PK, Austin JH, White CS, et al. Missed non-small cell lung cancer: radiographic findings of potentially resectable

lesions evident only in retrospect. *Radiology*. 2003;226(1):235-241.
94. Bayraktaroglu S, Savaş R, Basoglu OK, et al. Dynamic computed tomography in solitary pulmonary nodules. *J Comput Assist Tomogr*. 2008;32(2):222-227.
95. The American Thoracic Society and The European Respiratory Society. Pretreatment evaluation of non-small-cell lung cancer. *Am J Respir Crit Care Med*. 1997;156(1):320-332.
96. Seely JM, Mayo JR, Miller RR, Müller NL. T1 lung cancer: prevalence of mediastinal nodal metastases and diagnostic accuracy of CT. *Radiology*. 1993;186(1):129-132.
97. Tahara RW, Lackner RP, Graver LM. Is there a role for routine mediastinoscopy in patients with peripheral T1 lung cancers? *Am J Surg*. 2000;180(6):488-491.
98. Choi YS, Shim YM, Kim J, Kim K. Mediastinoscopy in patients with clinical stage I non-small cell lung cancer. *Ann Thorac Surg*. 2003;75(2):364-366.
99. Silvestri GA, Gould MK, Margolis ML, et al. Noninvasive staging of non-small cell lung cancer: ACCP evidence-based clinical practice guidelines (2nd edition). *Chest*. 2007;132(suppl 3):178S-201S.
100. Gould MK, Kuschner WG, Rydzak CE, et al. Test performance of positron emission tomography and computed tomography for mediastinal staging in patients with non-small-cell lung cancer: a meta-analysis. *Ann Intern Med*. 2003;139(11):879-892.
101. Dwamena BA, Sonnad SS, Angobaldo JO, Wahl RL. Metastases from non-small cell lung cancer: mediastinal staging in the 1990s—meta-analytic comparison of PET and CT. *Radiology*. 1999;213(2):530-536.
102. Shim SS, Lee KS, Chung MJ, Kim H, Kwon OJ, Kim S. Do hemodynamic studies of stage T1 lung cancer enable the prediction of hilar or mediastinal nodal metastasis? *AJR Am J Roentgenol*. 2006;186(4):981-988.
103. Reed CE, Harpole DH, Posther KE, et al; American College of Surgeons Oncology Group Z0050 trial. Results of the American College of Surgeons Oncology Group Z0050 trial: the utility of positron emission tomography in staging potentially operable non-small cell lung cancer. *J Thorac Cardiovasc Surg*. 2003;126(6):1943-1951.
104. Aberle DR, Adams AM, Berg CD, et al; National Lung Screening Trial Research Team. Reduced lung-cancer mortality with low-dose computed tomographic screening. *N Engl J Med*. 2011;365(5):395-409.
105. Vansteenkiste JF, Stroobants SS. PET scan in lung cancer: current recommendations and innovation. *J Thorac Oncol*. 2006;1(1):71-73.
106. Gould MK, Maclean CC, Kuschner WG, Rydzak CE, Owens DK. Accuracy of positron emission tomography for diagnosis of pulmonary nodules and mass lesions: a meta-analysis. *JAMA*. 2001;285(7):914-924.
107. Fletcher JW, Kymes SM, Gould M, et al; VA SNAP Cooperative Studies Group. A comparison of the diagnostic accuracy of 18F-FDG PET and CT in the characterization of solitary pulmonary nodules. *J Nucl Med*. 2008;49(2):179-185.
108. Jeong SY, Lee KS, Shin KM, et al. Efficacy of PET/CT in the characterization of solid or partly solid solitary pulmonary nodules. *Lung Cancer*. 2008;61(2):186-194.
109. Yi CA, Lee KS, Kim BT, et al. Tissue characterization of solitary pulmonary nodule: comparative study between helical dynamic CT and integrated PET/CT. *J Nucl Med*. 2006;47(3):443-450.
110. Bar-Shalom R, Kagna O, Israel O, Guralnik L. Noninvasive diagnosis of solitary pulmonary lesions in cancer patients based on 2-fluoro-2-deoxy-D-glucose avidity on positron emission tomography/computed tomography. *Cancer*. 2008;113(11):3213-3221.
111. Kagna O, Solomonov A, Keidar Z, et al. The value of FDG-PET/CT in assessing single pulmonary nodules in patients at high risk of lung cancer. *Eur J Nucl Med Mol Imaging*. 2009;36(6):997-1004.
112. Kim SK, Allen-Auerbach M, Goldin J, et al. Accuracy of PET/CT in characterization of solitary pulmonary lesions. *J Nucl Med*. 2007;48(2):214-220.
113. Shin KM, Lee KS, Shim YM, et al. FDG PET/CT and mediastinal nodal metastasis detection in stage T1 non-small cell lung cancer: prognostic implications. *Korean J Radiol*. 2008;9(6):481-489.
114. Kim BT, Lee KS, Shim SS, et al. Stage T1 non-small cell lung cancer: preoperative mediastinal nodal staging with integrated FDG PET/CT—a prospective study. *Radiology*. 2006;241(2):501-509.
115. Herder GJ, Golding RP, Hoekstra OS, et al. The performance of (18)F-fluorodeoxyglucose positron emission tomography in small solitary pulmonary nodules. *Eur J Nucl Med Mol Imaging*. 2004;31(9):1231-1236.
116. Pastorino U, Bellomi M, Landoni C, et al. Early lung-cancer detection with spiral CT and positron emission tomography in heavy smokers: 2-year results. *Lancet*. 2003;362(9384):593-597.
117. Nomori H, Watanabe K, Ohtsuka T, Naruke T, Suemasu K, Uno K. Evaluation of F-18 fluorodeoxyglucose (FDG) PET scanning for pulmonary nodules less than 3 cm in diameter, with special reference to the CT images. *Lung Cancer*. 2004;45(1):19-27.
118. Lindell RM, Hartman TE, Swensen SJ, et al. Lung cancer screening experience: a retrospective review of PET in 22 non-small cell lung carcinomas detected on screening chest CT in a high-risk population. *AJR Am J Roentgenol*. 2005;185(1):126-131.
119. Marom EM, Sarvis S, Herndon JE 2nd, Patz EF Jr. T1 lung cancers: sensitivity of diagnosis with fluorodeoxyglucose PET. *Radiology*. 2002;223(2):453-459.
120. Cheran SK, Nielsen ND, Patz EF Jr. False-negative findings for primary lung tumors on FDG positron emission tomography: staging and prognostic implications. *AJR Am J Roentgenol*. 2004;182(5):1129-1132.
121. Chun EJ, Lee HJ, Kang WJ, et al. Differentiation between malignancy and inflammation in pulmonary ground-glass nodules: the feasibility of integrated (18)F-FDG PET/CT. *Lung Cancer*. 2009;65(2):180-186.
122. Tsushima Y, Tateishi U, Uno H, et al. Diagnostic performance of PET/CT in differentiation of malignant and benign non-solid solitary pulmonary nodules. *Ann Nucl Med*. 2008;22(7):571-577.
123. Kim TJ, Park CM, Goo JM, Lee KW. Is there a role for FDG PET in the management of lung cancer manifesting predominantly as ground-glass opacity? *AJR Am J Roentgenol*. 2012;198(1):83-88.
124. Zou Y, Zhang M, Wang Q, Shang D, Wang L, Yu G. Quantitative investigation of solitary pulmonary nodules: dynamic contrast-enhanced MRI and histopathologic analysis. *AJR Am J Roentgenol*. 2008;191(1):252-259.
125. Kono R, Fujimoto K, Terasaki H, et al. Dynamic MRI of solitary pulmonary nodules: comparison of enhancement patterns of malignant and benign small peripheral lung lesions. *AJR Am J Roentgenol*. 2007;188(1):26-36.
126. Ohno Y, Koyama H, Takenaka D, et al. Dynamic MRI, dynamic multidetector-row computed tomography (MDCT), and coregistered 2-[fluorine-18]-fluoro-2-deoxy-D-glucose-positron emission tomography (FDG-PET)/CT: comparative study of capability for management of pulmonary nodules. *J Magn Reson Imaging*. 2008;27(6):1284-1295.